N-linked glycosylation is required for optimal proteolytic activation of membrane-bound transcription factor CREB-H

Chi-Ping Chan[1], To-Yuen Mak[1], King-Tung Chin[1,*], Irene Oi-Lin Ng[2] and Dong-Yan Jin[1,‡]

[1]Department of Biochemistry and [2]Department of Pathology, The University of Hong Kong, Faculty of Medicine Building, 21 Sassoon Road, Pokfulam, Hong Kong

*Present address: The Kimmel Center for Biology and Medicine at the Skirball Institute, New York University School of Medicine, New York, NY 10016, USA
‡Author for correspondence (dyjin@hkucc.hku.hk)

Accepted 10 February 2010
Journal of Cell Science 123, 1438-1448

doi:10.1242/jcs.067819

Summary

CREB-H is a liver-enriched bZIP transcription factor of the CREB3 subfamily. CREB-H is activated by intramembrane proteolysis that removes a C-terminal transmembrane domain. Aberrant expression of CREB-H is implicated in liver cancer. In this study we characterized N-linked glycosylation of CREB-H in the luminal domain at the C-terminus. We found that CREB-H is modified at three N-linked glycosylation sites in this region. Disruption of all three sites by site-directed mutagenesis completely abrogated N-linked glycosylation of CREB-H. The unglycosylated mutant of CREB-H was not unstable, unfolded or aggregated. Upon stimulation with an activator of intramembrane proteolysis such as brefeldin A and KDEL-tailed site 1 protease, unglycosylated or deglycosylated CREB-H was largely uncleaved, retained in an inactive form in the endoplasmic reticulum, and less capable of activating transcription driven by unfolded protein response element or C-reactive protein promoter. Taken together, our findings suggest that N-linked glycosylation is required for full activation of CREB-H through intramembrane proteolysis. Our work also reveals a novel mechanism for the regulation of CREB-H-dependent transcription.

Key words: Regulated intramembrane proteolysis, Membrane-bound transcription factors, Liver-enriched transcription factors, bZIP transcription factors, N-linked glycosylation, CREB-H, Endoplasmic reticulum, Unfolded protein response

Introduction

The liver carries out a wide range of functions such as metabolism and detoxification. Coordination of liver-specific functions is accomplished through a complex regulatory network that controls the expression of a repertoire of liver-specific genes (Duncan, 2000; Costa et al., 2003). At the core of this network are liver-enriched transcription factors (LETFs) and their tightly regulated activation in time and space is crucial to hepatic development, differentiation and function (Schrem et al., 2002; Schrem et al., 2004). While some LETFs such as hepatocyte nuclear factors (HNF) and CAATT enhancer-binding proteins (C/EBP) have been well characterized, CREB-H (also known as CREB3L3) is a newly identified LETF (Omori et al., 2001; Chin et al., 2005) and its physiological roles and regulation remain to be further investigated.

CREB-H is a bZIP protein of the CREB3 subfamily and it shares significant homology with LZIP (CREB3), the prototypic member of the subfamily (Freiman and Herr, 1997; Lu et al., 1997; Jin et al., 2000). In addition to the DNA-binding and dimerization domains characteristic of bZIP proteins (Vinson et al., 2006), CREB-H also possesses a transmembrane domain at the proximal C-terminal side of the bZIP domain and thus localizes to the endoplasmic reticulum (ER) (Chin et al., 2005; Zhang et al., 2006). In response to a poorly defined upstream signal that is thought to be related to ER stress (Bailey et al., 2007; Llarena et al., 2010), CREB-H is activated by regulated intramembrane proteolysis (RIP) that releases its N-terminal part for nuclear translocation and transcriptional activation (Omori et al., 2001; Chin et al., 2005). Proteolytic activation of other members of the CREB3 subfamily such as LZIP, OASIS (CREB3L1), BBF2H7 (CREB3L2) and CREB3L4 has also been characterized (Raggo et al., 2002; Kondo et al., 2005; Kondo et al., 2007; Stirling and O'Hare, 2006). Because these transcription factors are critically involved in inflammatory response, iron homeostasis, bone formation and chondrocyte differentiation (Zhang et al., 2006; Murakami et al., 2009; Saito et al., 2009; Vecchi et al., 2009), it is of great interest to elucidate the mechanisms that subserve their regulation by RIP. In a more general sense, RIP is an important mechanism for the regulation of other membrane-anchored transcription factors (Brown et al., 2000). For instance, RIP of SREBP and ATF6 has been extensively studied (Bailey and O'Hare, 2007; Bengoechea-Alonso and Ericsson, 2007). The activation of SREBP plays a central role in sterol homeostasis (Brown and Goldstein, 1997), whereas proteolysis of ATF6 serves as a critical switch in unfolded protein response (UPR) (Haze et al., 1999; Ye et al., 2000). In view of this, an understanding of how proteolytic activation of CREB-H is regulated might shed significant light on its biological function.

CREB-H has been implicated in linking ER stress to acute phase response (APR) and iron metabolism (Zhang et al., 2006; Luebke-Wheeler et al., 2008; Vecchi et al., 2009). APR is a nonspecific systemic reaction to disturbances in homeostasis such as tissue injury, inflammation and malignant tumors (Gabay and Kushner, 1999). Pro-inflammatory cytokines such as tumor necrosis factor α (TNF-α), interleukin 1 (IL-1), and IL-6 are important mediators of APR (Moshage, 1997). In response to these cytokines, hepatic production of acute phase proteins such as C-reactive

Journal of Cell Science

protein (CRP) and serum amyloid A is elevated to more than 1000-fold (Mortensen, 2001). The expression of hepcidin, a peptide hormone that controls iron homeostasis, is also induced during inflammation (Lee and Beutler, 2009). While CREB-H is known to activate the CRP and hepcidin promoters (Zhang et al., 2006; Vecchi et al., 2009), it is not clear through what mechanism CREB-H could respond to pro-inflammatory cytokines and other stimuli to effect transcriptional activation.

The activity of various transcription factors is commonly regulated through posttranslational modifications (Seet et al., 2006). Glycosylation is a major form of posttranslational modification and its regulatory roles in the context of different transcription factors such as CREB, NF1C, Oct-2, Sp1 and STAT5 have been documented (Jackson and Tjian, 1988; Kane et al., 2002; Lamarre-Vincent and Hsieh-Wilson, 2003; Gewinner et al., 2004; Ahmad et al., 2006). In addition, ATF6, another membrane-bound bZIP transcription factor activated by RIP in response to ER stress, is also known to be N-linked glycosylated and this modification has an impact on its transcriptional activity (Hong et al., 2004). Particularly, unglycosylated ATF6 mutants exhibit a faster rate of transport to the Golgi apparatus, leading ultimately to constitutive nuclear localization and transcriptional activation in the absence of ER stress (Hong et al., 2004). This illustrates the importance of N-linked glycosylation in regulating the activity of membrane-bound transcription factors and prompted us to investigate whether CREB-H might also be N-linked glycosylated.

We have previously characterized CREB-H for its proteolytic activation and growth suppressive activity. In addition, posttranslational modification of CREB-H has also been suggested in our analysis of native and recombinant CREB-H proteins (Chin et al., 2005). In this study, we extended our work to characterize N-linked glycosylation of CREB-H. CREB-H was found to be N-linked glycosylated at three sites in the luminal domain. Abrogation of this modification rendered CREB-H significantly less active in transcriptional activation, pointing to a role in optimal proteolytic cleavage. Our findings reveal a novel regulatory mechanism in CREB-H-dependent transcription and have implications in hepatic physiology and pathology.

Results

CREB-H is glycosylated in the C-terminal region

We and others have previously noticed that CREB-H has a higher than expected apparent molecular mass in SDS-PAGE gels (Chin et al., 2005; Zhang et al., 2006). Further analysis with glycosylation inhibitor and endoglycosidic enzymes has revealed that CREB-H is N-linked glycosylated (Bailey et al., 2007). To verify N-linked glycosylation of CREB-H in the C-terminal luminal domain we also made use of endoglycosidic enzymes that can specifically and efficiently remove N-linked oligosaccharides from glycoproteins. Two of these endoglycosidases, Endo-H and PNGase F, were employed to treat the lysates of HEK293T cells transfected with CREB-H WT and CREB-HΔTC. CREB-HΔTC is a truncated mutant consisting of amino acids 1-318, in which the transmembrane and C-terminal domains had been removed (Chin et al., 2005). When we performed western blotting with anti-V5 to probe for the V5-tagged CREB-H proteins, a significant decrease in the apparent molecular mass of full-length CREB-H WT protein was noted upon treatment with either Endo-H (supplementary material Fig. S1A, lane 2 compared with lane 1) or PNGase F (supplementary material Fig. S1B, lane 2 compared with lane 1), while there was no observable change for CREB-HΔTC after the same treatment (supplementary material Fig. S1A and S1B, lanes 3-4). Hence, in agreement with a previous report (Bailey et al., 2007), these results indicated that N-linked glycosylation did occur in CREB-H and the site(s) for N-linked glycosylation would be located in the C-terminal region of CREB-H that is missing in the CREB-HΔTC mutant.

To verify N-linked glycosylation of CREB-H in the liver, we used anti-CREB-H serum α-CH9 to detect endogenous CREB-H protein in the lysates of mouse liver tissue. Because the steady-state level of CREB-H was low in the liver, we first concentrated CREB-H by co-immunoprecipitation with α-CH9. A fast-migrating protein band reactive to α-CH9 but not to pre-immune serum was evident in the Endo-H-treated proteins precipitated with α-CH9 (supplementary material Fig. S1C, lane 2 compared with lanes 1, 3 and 4). Thus, endogenous CREB-H was also N-linked glycosylated in the liver.

Determination of N-linked glycosylation sites

Next, we set out to map the exact site(s) for N-linked glycosylation in CREB-H. The consensus sequence for N-linked glycosylation sites consists of Asn-x-Ser/Thr, where x denotes any amino acid except proline (Bause, 1983). Four N-linked glycosylation sites within the luminal domain of human CREB-H were previously predicted (Bailey et al., 2007), but only three of them are conserved in human and mouse CREB-H. These three conserved sites (Fig. 1A) were chosen for further investigation. Site-directed mutagenesis was carried out to change the conserved threonine residue at each of these sites into isoleucine to produce point mutants designated m1 (T413I), m2 (T420I) and m3 (T427I). Additional mutants with all different combinations of these three mutations were also created. Western blot analysis was then performed to check for glycosylation in CREB-H through PNGase F (Fig. 1B) and Endo-H (Fig. 1C) treatment.

N-linked glycosylation in CREB-H causes an increase in molecular mass that can be detected as a mobility shift in SDS-PAGE. In line with this, CREB-H WT moved the slowest in SDS-PAGE (Fig. 1B, lane 1; Fig. 1C, lane 1) while the triple mutant of CREB-H (m1+2+3), in which all three glycosylation sites had been disrupted, moved the fastest (Fig. 1B, lane 15; Fig. 1C, lane 3). The mobility of CREB-H single and double mutants was intermediate. In order to verify that N-linked glycosylation is responsible for the observed mobility shift, lysates of transiently transfected cells were also subjected to PNGase F or Endo-H treatment before SDS-PAGE. It was found that the apparent molecular mass of CREB-H WT dropped most dramatically after the treatment with PNGase F or Endo-H. Upon the same treatment, the decrease in molecular mass was progressively less pronounced as more of the three sites were disrupted in the CREB-H mutant. Notably, no difference was detected in CREB-H m1+2+3 before and after endoglycosidase treatment (Fig. 1B, lanes 15 and 16; Fig. 1C, lanes 3 and 4). The slight difference between the apparent molecular mass of Endo-H-treated CREB-H WT and that of CREB-H m1+2+3 (Fig. 1C, lane 2 compared with lane 4) was probably due to incomplete deglycosylation of CREB-H WT. Nevertheless, CREB-H was N-linked glycosylated at all three sites within the luminal domain and disruption of these sites completely abrogated N-linked glycosylation of CREB-H.

CREB-H glycosylation mutants were poor activators of transcription

Since we have confirmed and mapped the three N-linked glycosylation sites in CREB-H, we next asked whether N-linked

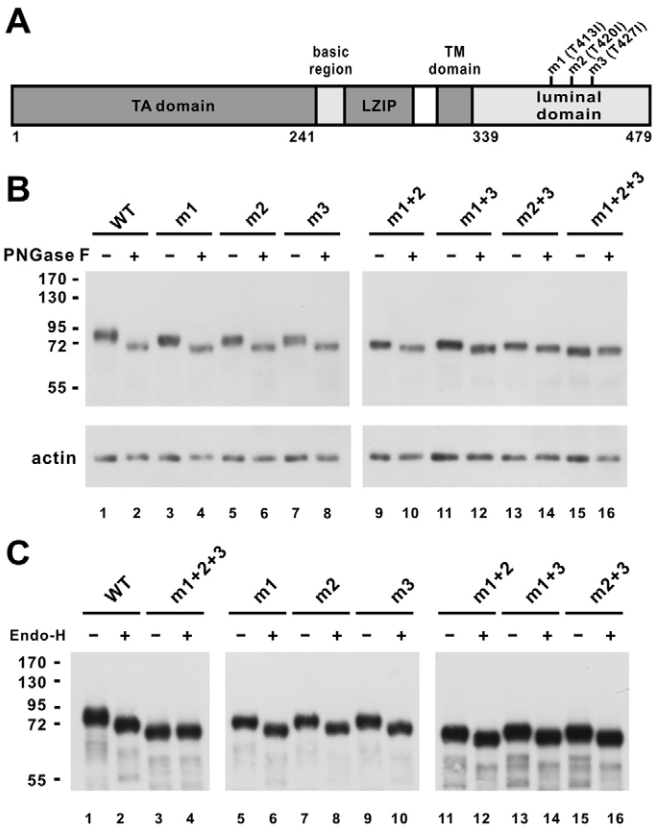

Fig. 1. N-linked glycosylation status of CREB-H and its glycosylation mutants. (**A**) Schematic representation of the structure of mouse CREB-H. Mutated N-linked glycosylation sites m1 (T413I), m2 (T420I) and m3 (T427I) are indicated. (**B**,**C**) Western blot analysis. HEK293T cells transfected with plasmids expressing the indicated forms of CREB-H were treated with PNGase F (B) and Endo-H (C). Western blotting was performed with α-V5.

glycosylation influenced the function of CREB-H. To address this question, we performed a series of dual luciferase reporter assay. The ability of CREB-H WT and CREB-H glycosylation mutants to activate UPR element (UPRE)- and CRP-promoter-driven transcription was analyzed. CRP has previously been shown to be a physiological target of CREB-H (Zhang et al., 2006). The luciferase reporters used were pUPRE-Luc, which harbors six copies of the consensus UPRE (Wang et al., 2000), and pCRP-Luc, which contains –1834 to +150 of the human CRP promoter (Nishikawa et al., 2008).

For CREB-H to activate transcription, it has to undergo proteolytic activation and nuclear translocation. Because N-linked glycosylation occurs in the luminal domain, which is removed by intramembrane proteolysis, both CREB-H WT and its glycosylation mutants might generate the same active form after proteolytic activation. Plausibly, a difference between CREB-H WT and its glycosylation mutants in their ability to activate the UPRE or CRP promoter probably indicates a difference in or before proteolysis.

When HepG2 cells were transfected with UPRE reporter, CREB-H WT induced a more than sixfold activation on UPRE whereas the glycosylation mutants showed progressively decreasing activity (Fig. 2A). As such, CREB-H m1+2+3 remained half as active as CREB-H WT (Fig. 2A). In HepG2 cells transfected with a reporter driven by CRP promoter, CREB-H WT induced threefold activation whereas the mutants exhibited progressively decreasing activity as one to three N-linked glycosylation sites were mutated (Fig. 2B). It was noteworthy that CREB-H m1+2+3 had lost its ability to activate CRP promoter. In Hep3B cells transfected with UPRE reporter, the activity of CREB-H m1+2+3 was reduced even more dramatically to a level that was comparable with the vector control, whereas CREB-H WT produced a sevenfold activation (Fig. 2C). In all three cases, the differences between CREB-H WT and CREB-H m1+2+3 were statistically very significant (Fig. 2A-C).

As shown in Fig. 1, the expression levels of CREB-H WT and mutants were not significantly different in HEK293T cells. Similar results were also obtained from HepG2 and Hep3B cells (data not shown). Thus, the differences in transcriptional activity between CREB-H WT and mutants could probably not be explained by variations in protein expression levels. In particular, no difference could be detected in the expression levels of CREB-H WT and CREB-H m1+2+3 in Hep3B cells (Fig. 2D). In addition, trace amount of cleavage product, the size of which is generally consistent with that predicted for the active form of CREB-H, was also detected in Hep3B cells expressing CREB-H WT, but not CREB-H m1+2+3 (Fig. 2D). This supports the notion that the transcriptional activity detected ambiently in HepG2 and Hep3B cells overexpressing CREB-H WT (Fig. 2A-C) was likely attributed to a basal level of constitutive cleavage of CREB-H. By the same reasoning, the inability to activate UPRE and CRP promoter by CREB-H m1+2+3 was probably due to reduced level of the active N-terminal fragment of CREB-H in the nucleus.

The above results were obtained with transiently transfected reporter constructs. To verify the differential activity of CREB-H WT and CREB-H m1+2+3 in activating cell-endogenous CRP promoter, we compared the levels of CRP transcript in HepG2 cells expressing CREB-H WT, CREB-HΔTC and CREB-H m1+2+3 (Fig. 2E). The level of endogenous CREB-H in HepG2 cells was undetectable (Chin et al., 2005). In addition, CRP was not expressed in mock-transfected HepG2 cells (Fig. 2E, lane 1). Thus, the detection of CRP transcript in transfected cells would be solely attributed to the expression of exogenously introduced CREB-H protein. Consistent with this idea, CRP transcript was detected weakly in cells expressing CREB-H WT (Fig. 2E, lane 2). The abundance of CRP mRNA was higher in cells expressing CREB-HΔTC, a constitutively active mutant (Fig. 2E, lane 3). However, CRP transcript was not found in cells expressing CREB-H m1+2+3 (Fig. 2E, lane 4). Hence, N-linked glycosylation of CREB-H was probably required for its ability to activate CRP expression. Furthermore, this requirement of N-linked glycosylation for full activation of CREB-H probably occurs at a step before or during intramembrane proteolysis.

Unglycosylated CREB-H protein was not unstable, unfolded or aggregated

The influence of N-linked glycosylation on CREB-H function prompted us to investigate further the underlying mechanism. Provided that N-linked glycosylation is required in or before proteolytic activation as discussed above, we tested the possibility that CREB-H m1+2+3 is an unstable or unfolded protein. Because the steady-state amounts of underglycosylated mutants of CREB-H in cultured cells were not subtly reduced compared with CREB-H WT (Fig. 1B,C), their differential activity was not likely to be due to protein turnover. To address this issue, we compared the turnover of CREB-H WT and CREB-H m1+2+3 proteins in HepG2 cells treated with DMSO or cycloheximide (Fig. 3A,B). When

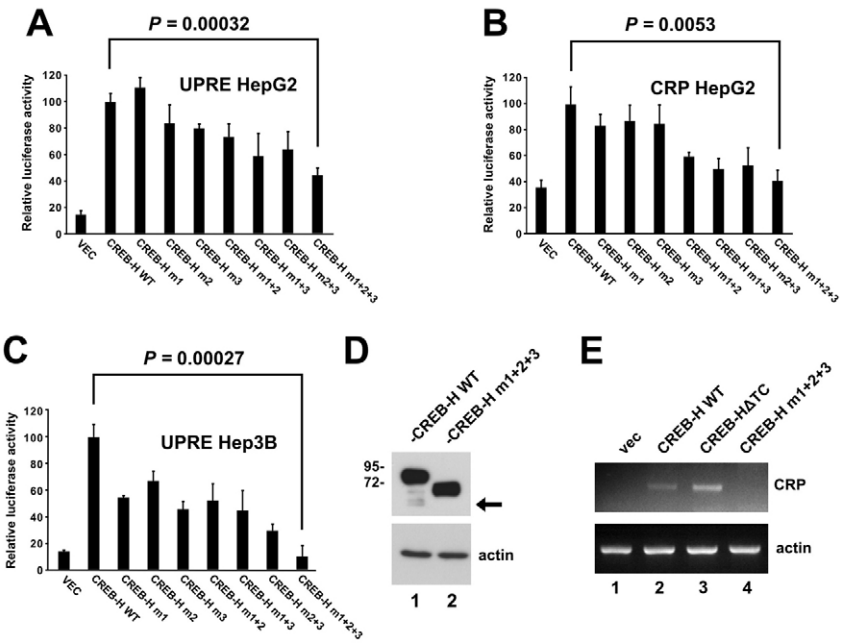

Fig. 2. Transcriptional activity of CREB-H and its glycosylation mutants. (**A-C**) Luciferase reporter assays. Empty vector (VEC) and plasmids (0.3 μg each) expressing CREB-H and its mutants, as indicated, were individually co-transfected with either pUPRE-Luc (A,C) or pCRP-Luc (B) reporter plasmid (0.2 μg) into HepG2 (A,B) and Hep3B (C) cells. An SV40 promoter-driven *Renilla* luciferase plasmid was also transfected into the cells. The cell lysates were measured for firefly luciferase luminescence and the readings were normalized to the luminescence of *Renilla* luciferase. Results are representative of three independent experiments and error bars indicate the s.d. Differences between CREB-H WT and CREB-H m1+2+3 are statistically very significant as evaluated by Student's *t*-test. *P* values are as indicated. (**D**) Western blot analysis. Expression of CREB-H WT and CREB-H m1+2+3 in Hep3B cells was verified by western blotting with α-myc. The arrow indicates the cleaved form of CREB-H. Cells were treated with 10 μM MG-132 before harvest. (**E**) RT-PCR analysis of CRP transcript. Total RNA from HepG2 cells transfected with plasmids expressing the indicated forms of CREB-H was extracted and subjected to DNase treatment. RT-PCR was performed with 5 μg RNA to assess the expression of endogenous CRP and β-actin transcripts.

protein synthesis was inhibited by cycloheximide, the amount of CREB-H WT diminished significantly within 30 minutes (Fig. 3B, lane 3 compared with lane 1). At 4 hours after treatment, CREB-H WT was almost undetectable (Fig. 3B, lane 6). By contrast, significant amount of CREB-H m1+2+3 was still found 4 hours after treatment with cycloheximide (Fig. 3B, lane 12). As such, the half-life of CREB-H m1+2+3 (7.3 hours) was significantly longer than that of CREB-H WT (1.3 hours; Fig. 3C). Thus, whereas CREB-H WT protein had a fast turnover, CREB-H m1+2+3 was more stable. In other words, loss of N-linked glycosylation did not destabilize CREB-H protein. The amounts of CREB-H WT in the absence of cycloheximide (Fig. 3A, lanes 3-6) did not drop substantially, suggesting that new protein might be synthesized to maintain the steady-state level of CREB-H in the cell.

Suppose that CREB-H m1+2+3 was an unfolded protein retained in the ER, its accumulation would activate UPR (Ron and Walter, 2007). However, overexpression of CREB-H m1+2+3 in HepG2 and Hep3B cells was not found to activate UPRE, which is an indicator of UPR (Fig. 2A,C). Hence, CREB-H m1+2+3 was neither an unstable nor an unfolded protein.

Additionally, to shed light on whether CREB-H m1+2+3 is aggregated, we also compared the electrophoretic mobility patterns of CREB-H WT and CREB-H m1+2+3 on non-denaturing polyacrylamide gels. Since the migration patterns of CREB-H WT and CREB-H m1+2+3 on the non-denaturing gel were similar and an aggregated form of CREB-H m1+2+3 was not detected (data not shown), it is unlikely that aggregation of CREB-H m1+2+3 occurs in cultured HepG2 cells.

Brefeldin A induces proteolytic activation of CREB-H

As a first step to explore the possibility that the reduced activity of CREB-H mutants defective for N-linked glycosylation in the luminal domain might be attributed to an inhibition of proteolytic activation, we induced intramembrane proteolysis of CREB-H with brefeldin A (BFA).

BFA is a drug that induces the fusion of ER and the Golgi complex (Lippincott-Schwartz et al., 1989). It is well-known that S1P and site-2-protease (S2P) are located in the Golgi and they catalyze proteolysis of CREB-H (Zhang et al., 2006). Since CREB-H localizes predominantly to the ER membranes (Omori et al., 2001; Chin et al., 2005) whereas S1P and S2P are found in the Golgi, they cannot encounter one another in the absence of stimuli. Only in response to specific activators, does CREB-H translocate from ER to Golgi and is consequently cleaved by S1P and S2P. With the addition of BFA, the fusion of ER and Golgi enforces the action of S1P and S2P on CREB-H, leading to constitutive activation of transcriptional activity (Zhang et al., 2006). Consistent with this notion, our results from luciferase assays indicated that the activity of CREB-H WT on UPRE was significantly increased upon the addition of BFA to HepG2 cells (Fig. 4A). This was probably due to BFA-induced proteolytic cleavage of CREB-H. By contrast, the constitutively active CREB-HΔTC mutant did not respond to BFA (Fig. 4A). For CREB-H m1+2+3, the activation induced by BFA was significantly reduced (Fig. 4A). This suggested that CREB-H unglycosylated mutants might be poor substrates of S1P and S2P.

It was thought that inducers of UPR, such as tunicamycin (Tu) and thapsigargin (Tg), might also induce proteolytic activation of CREB-H (Zhang et al., 2006; Luebke-Wheeler et al., 2008; Vecchi et al., 2009). On the contrary, Tu was also shown to have no effect on proteolytic cleavage of CREB-H (Bailey et al., 2007) and was unable to induce its translocation into the nucleus (Llarena et al., 2010). Furthermore, because Tu is a glycosylation inhibitor, it was expected to inhibit CREB-H activation in our model. To clarify this issue, we treated HepG2 cells with Tu and Tg and then checked for CREB-H glycosylation and activity. Whereas treatment with Tu inhibited glycosylation of CREB-H leading to the appearance of fast-migrating hypoglycosylated species, addition of Tg had no influence on CREB-H glycosylation (Fig. 4B, lanes 3 and 4 compared with lanes 1 and 2). Interestingly, whereas both Tu and Tg activated ATF6-dependent transcription from UPRE, Tu significantly inhibited and Tg had no influence on CREB-H-dependent activation (Fig. 4C). Additionally, neither Tu nor Tg affected the activity of CREB-H m1+2+3. Thus, Tu was able to inhibit transcriptional activity of CREB-H, which was plausibly mediated through inhibition of glycosylation. Our results were at

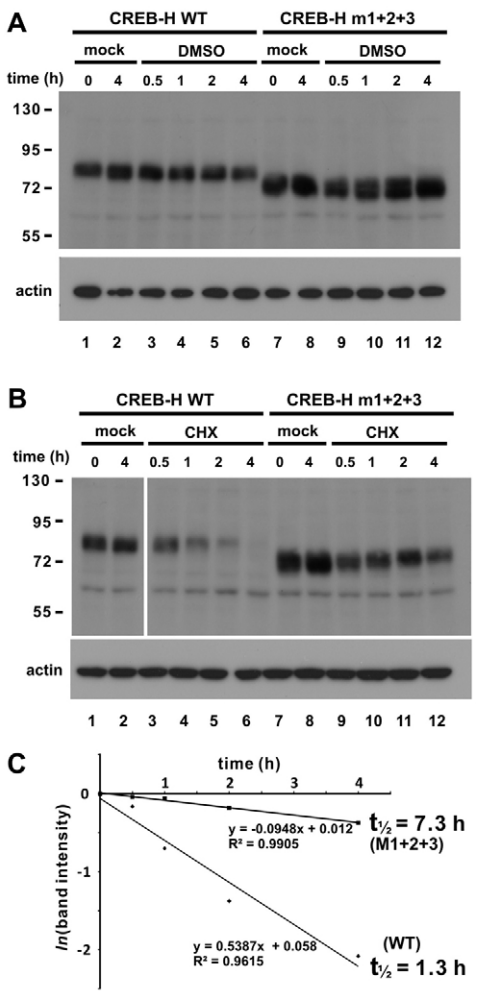

Fig. 3. Protein stability of CREB-H WT and CREB-H m1+2+3. (**A**,**B**) HepG2 cells were transfected with pcDNA-CREB-H (lanes 1-6) or pcDNA-CREB-H m1+2+3 (lanes 7-12) for 48 hours. Cells were mock treated (lanes 1, 2, 7 and 8) or treated with dimethyl sulfoxide (DMSO; A, lanes 3-6 and 9-12) or 200 μM cycloheximide (CHX; B: lanes 3-6 and 9-12) for the indicated duration before harvest. Western blotting was performed with α-V5. β-actin was also probed to control for equal loading. (**C**) Half-lives ($t_{1/2}$) of CREB-H WT and CREB-H m1+2+3 were calculated as described by Bachmair et al. (Bachmair et al., 1986).

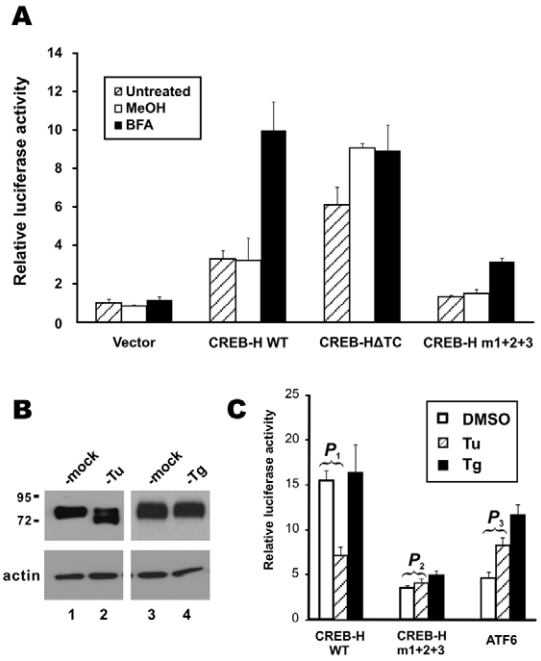

Fig. 4. Activation of CREB-H transcriptional activity by BFA. (**A**) Effect of BFA. Empty vector and plasmids (0.3 μg each) expressing CREB-H, CREB-HΔTC and CREB-H m1+2+3 were individually co-transfected with pCRP-Luc plasmid (0.2 μg) into HepG2 cells. Cells were untreated, mock-treated with methanol (MeOH), or stimulated with BFA. Luciferase activity was measured as in Fig. 2. (**B**) Effect of Tu and Tg on CREB-H glycosylation. HepG2 cells were transfected with pcDNA-CREB-H. Cells were mock treated or treated with Tu or Tg. Cell lysates were analyzed by western blotting with α-myc. To ensure equal loading, β-actin was also probed. (**C**) Effect of Tu and Tg on CREB-H activity. HepG2 cells were transfected with plasmids expressing CREB-H, CREB-H m1+2+3 and ATF6 separately. Cells were also co-transfected with pUPRE-Luc. Cells were then mock treated with DMSO or treated with Tu or Tg. Luciferase assay was performed as in Fig. 2. All readings were normalized to those of the vector control. Treatment with Tu significantly inhibits transcriptional activity of CREB-H (P_1=0.0051, Student's *t*-test) but activates that of ATF6 (P_3=0.0051). In the control experiment, Tu has no significant effect on the activity of CREB-H m1+2+3 (P_2=0.068).

odds with previous findings that Tu either increased (Zhang et al., 2006) or had no effect (Bailey et al., 2007) on proteolytic activation of CREB-H. However, a more careful re-analysis of published data indicated that our observations are more in keeping with results reported by Bailey et al. (Bailey et al., 2007), in which both constitutive and BFA-induced cleavage of CREB-H was less pronounced in the presence of Tu [see figures S3 and S4 in Bailey et al. (Bailey et al., 2007)].

Unglycosylated CREB-H does not translocate to the nucleus upon activation by BFA

Tu was able to induce almost complete deglycosylation of CREB-H, but it either stimulated (Zhang et al., 2006) or had no influence (Bailey et al., 2007) on proteolytic cleavage of CREB-H in the absence of BFA. In addition, Tu did not induce nuclear translocation of CREB-H (Llarena et al., 2010) and might exert a moderate inhibitory effect on BFA-induced cleavage of CREB-H (Bailey et al., 2007). In light of these discrepancies, the use of our unglycosylated CREB-H mutant should provide important clues to the impact of glycosylation on BFA-induced cleavage and consequent nuclear translocation of CREB-H.

To further investigate the fate of unglycosylated CREB-H, we compared the subcellular localization of CREB-H WT and its unglycosylated mutant CREB-H m1+2+3 in BFA-treated cells using confocal immunofluorescence microscopy. Because the active fragment of CREB-H is rapidly degraded in the nucleus, the proteosome inhibitor MG-132 was added to all cells. In the absence of BFA, both CREB-H WT and CREB-H m1+2+3 were detected in the cytoplasm (Fig. 5, panels 1-3 and 7-9). There was no observable difference between the two species. Importantly, aggregates of CREB-H m1+2+3 were not found in transfected cells (Fig. 5, panel 8).

As shown in our previous work (Chin et al., 2005), CREB-H colocalized perfectly with calnexin, consistent with targeting to the

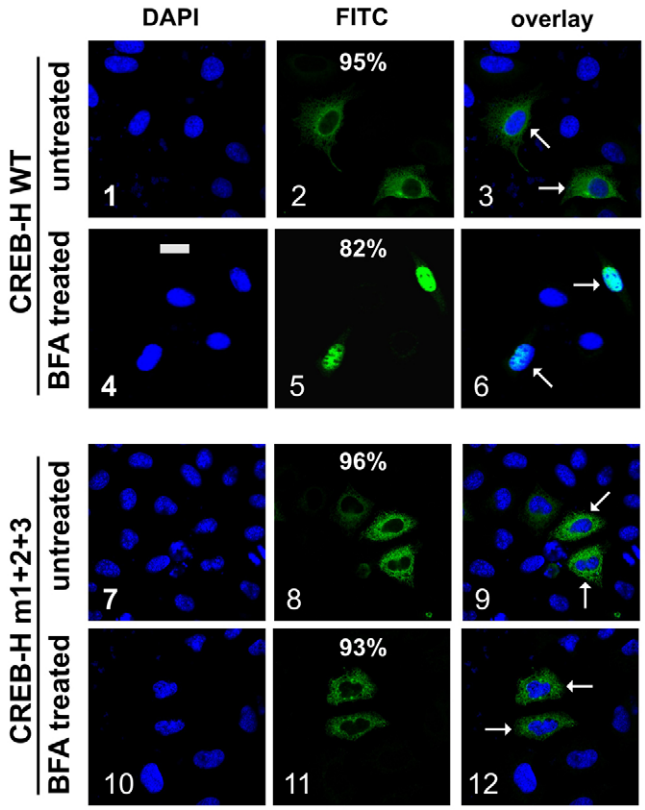

Fig. 5. Subcellular localization of CREB-H WT and CREB-H m1+2+3. The pCMV-CREB-H (panels 1-6) and pCMV-CREB-H m1+2+3 (panels 7-12) plasmids were separately transfected into HeLa cells. All cells were treated with 10 μM MG-132. Cells were either treated (panels 4-6 and 10-12) or not treated (panels 1-3 and 7-9) with BFA for 6 hours before harvest. Cells were then fixed and co-stained with α-myc (green, panels 2, 5, 8 and 11) and DAPI (blue, panels 1, 4, 7 and 10). Green (CREB-H) and blue (DAPI) fluorescent signals were then overlaid (panels 3, 6, 9 and 12). Colocalizations are shown in pale blue. The same fields are shown in panels 1-3, 4-6, 7-9 and 10-12. Arrows indicate transfected cells. Three independent experiments were carried out. Fifty transfected cells in each group were inspected and the average percentages of cells that showed the same localization pattern were indicated. The variations of percentages in the three experiments were within ±5% from the average. Scale bar: 20 μm.

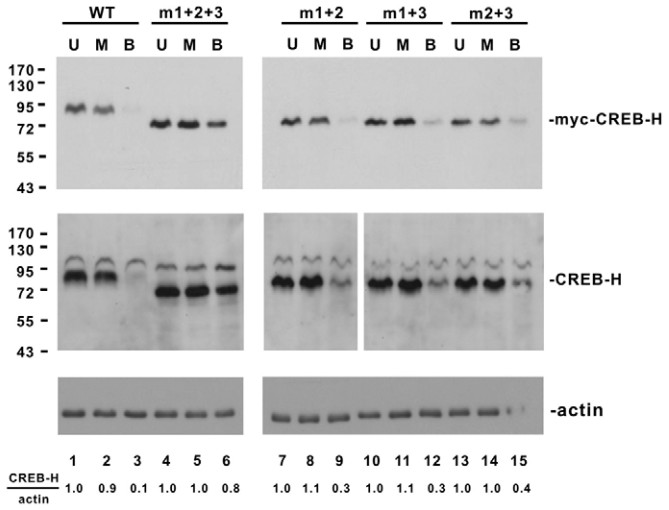

Fig. 6. BFA-induced proteolytic cleavage of CREB-H and mutants. HEK293T cells were transfected with pCMV-CREB-H (lanes 1-3), pCMV-CREB-H m1+2+3 (lanes 4-6), pCMV-CREB-H m1+2 (lanes 7-9), pCMV-CREB-H m1+3 (lanes 10-12), pCMV-CREB-H m2+3 (lanes 13-15) for 48 hours. Cells were either untreated (lanes 1, 4, 7, 10 and 13) or treated with methanol (lanes 2, 5, 8, 11 and 14) or BFA (lanes 3, 6, 9, 12 and 15) for 6 hours before harvest. Cell lysates were analyzed by western blotting with α-myc (upper panels) or α-CREB-H (middle panels). Western blotting with anti-β-actin (lower panels) was also performed to verify equal loading. U, untreated; M, treated with methanol; B, treated with BFA. The ratios of CREB-H to β-actin (CREB-H/actin) were calculated by densitometry.

ER. Upon BFA treatment, CREB-H WT protein was found to have translocated to the nucleus (Fig. 5, panels 4-6). However, CREB-H m1+2+3 did not change its subcellular localization after BFA treatment and remained in the ER (Fig. 5, panels 10-12). These results suggested that CREB-H WT was readily activated by BFA and thus the active species accumulated in the nucleus upon BFA treatment. By contrast, CREB-H m1+2+3 might be less susceptible to induced cleavage by BFA so that a decreased amount of the active form was produced and thus the majority of CREB-H m1+2+3 protein was found in the ER.

Unglycosylated or deglycosylated CREB-H is less susceptible to proteolytic activation

To determine the reasons for the observed difference in subcellular localization of CREB-H WT and CREB-H m1+2+3, we performed western blot analysis using anti-myc and anti-CREB-H after the treatment with BFA. HEK293T cells were transfected with the expression plasmids for CREB-H WT and the glycosylation mutants. Some of the cells were subjected to the treatment with BFA before the cells were harvested while other cells in the control groups were either untreated or treated with methanol (Fig. 6). Interestingly, the steady-state amount of CREB-H WT was significantly reduced after BFA treatment whereas the abundance of CREB-H m1+2+3 did not change much (Fig. 6, lane 3 compared with lane 6). In addition, the amounts of the double mutants of CREB-H were intermediate after BFA treatment. Because the disappearance of CREB-H WT band in western blot after BFA treatment was probably due to rapid turnover of the active form, this lends some support to the notion that N-linked glycosylation is influential in the proteolytic activation of CREB-H.

To further confirm that the disappearance of CREB-H WT band and the reduced abundance of CREB-H double mutants after the treatment with BFA were really attributed to the proteolytic cleavage of CREB-H, we performed additional western blot analysis with anti-myc (Fig. 7; supplementary material Fig. S2). MG-132 was added to the cells to prevent proteasomal degradation of cleaved CREB-H. When HEK293T cells expressing CREB-H WT were treated with BFA for 1-6 hours, substantial amounts of CREB-H active form were found in the cell lysates (Fig. 7, lanes 3-6 compared with lanes 1 and 2). The molecular mass (approximately 52 kDa) of this form is generally consistent with the predicted size of the CREB-H cleavage product generated by S1P and S2P proteases. Notably, the amounts of the active form recovered from HEK293T cells expressing CREB-H m1+2+3 were considerably lower (Fig. 7, lanes 9-12). Hence, the cleavability of CREB-H WT by S1P and S2P proteases is significantly higher than that of CREB-H m1+2+3 in HEK293T cells.

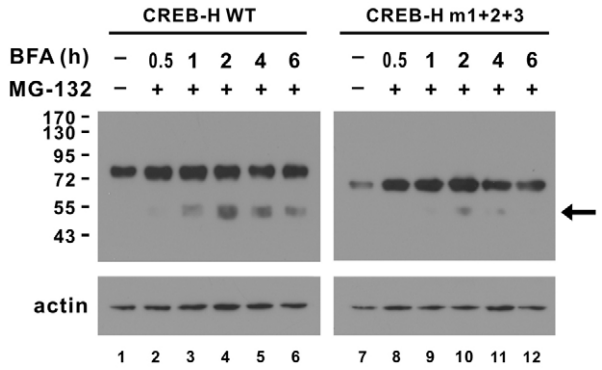

Fig. 7. Susceptibility of CREB-H WT and CREB-H m1+2+3 to BFA-induced cleavage. HEK293T cells were transfected with pCMV-CREB-H (lanes 1-6) and pCMV-CREB-H m1+2+3 (lanes 7-12) for 48 hours. Before harvest cells were treated with 5 μg/ml BFA and 10 μM MG-132 for the indicated duration. Cells in lanes 1 and 7 were mock treated with DMSO. Cell lysates were analyzed by western blotting with α-myc. The arrow indicates the cleaved form of CREB-H. β-actin was also probed to control for equal loading.

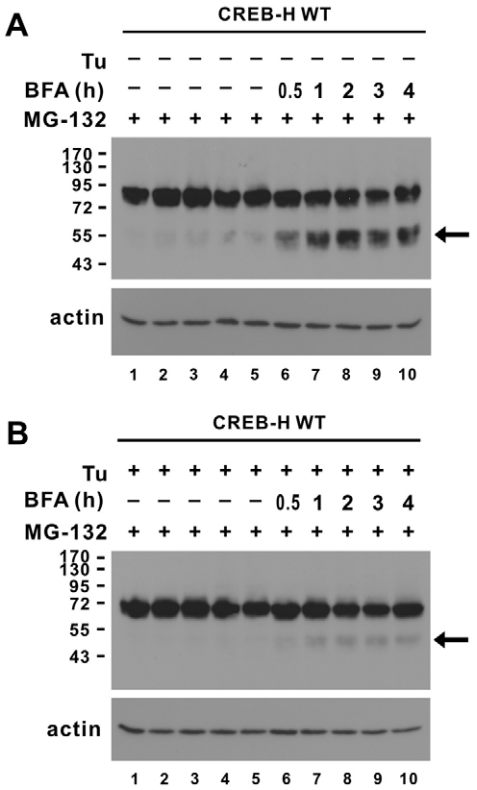

Fig. 8. Effect of deglycosylation on BFA-induced cleavage of CREB-H. HEK293T cells were transfected with pCMV-CREB-H for 48 hours. Before harvest cells were treated with (**A**) BFA plus MG-132 for the indicated duration, or (**B**) with 2 μg/ml Tu for 6 hours followed by BFA plus MG-132 for the indicated duration. Cell lysates were analyzed by western blotting with α-myc. The arrow indicates the cleaved form of CREB-H. β-actin was also probed to control for equal loading.

Similar experiments were also performed in COS-7 cells transfected with expression plasmids of CREB-H WT and CREB-H m1+2+3. Indeed, more CREB-H active form was observed in the lysate of COS-7 cells expressing CREB-H WT and treated with BFA and MG-132 (supplementary material Fig. S2, lane 4). By contrast, no significant amount of CREB-H active form could be detected in the CREB-H m1+2+3 group with or without treatment (supplementary material Fig. S2, lanes 5-8). This suggested that CREB-H WT was again much more susceptible to BFA-induced proteolytic cleavage than its unglycosylated mutant in COS-7 cells. Collectively, our results pointed to the importance of N-linked glycosylation in proteolytic activation of CREB-H.

Our demonstration of the substantially decreased susceptibility of unglycosylated CREB-H to S1P- and S2P-mediated proteolytic cleavage (Fig. 7; supplementary material Fig. S2) contradicts previous findings that Tu-induced deglycosylation of CREB-H has a stimulatory effect on proteolytic activation (Zhang et al., 2006). Although we observed a pronounced inhibition of CREB-H cleavage by Tu-induced deglycosylation, our data are more consistent with those of another group who reported no effect or at most a modest reduction in cleavage (Bailey et al., 2007). To clarify these discrepancies and to formally exclude the possibility that the decreased cleavability of our unglycosylated CREB-H mutant could be due to structural or non-structural changes other than the lack of glycosylation, we revisited the issue of Tu-induced deglycosylation of CREB-H.

When CREB-H-expressing HEK293T cells were treated with BFA and MG-132 in the absence of Tu, accumulation of CREB-H active form was observed as expected (Fig. 8A, lanes 6-10). In stark contrast, when the same experiment was repeated in the presence of Tu, the cleavage product of CREB-H detected was considerably less (Fig. 8B, lanes 6-10). Similar results were also obtained from HepG2 cells treated with Tu or not (supplementary material Fig. S3, lane 5 compared with lane 3). Hence, Tu-induced deglycosylation of CREB-H WT also resulted in significant inhibition of BFA-induced proteolytic cleavage. In other words, the substantially decreased cleavability seen with unglycosylated CREB-H mutant (Fig. 7) was probably not due to unexpected effects caused by the mutation of the three asparagines in the luminal domain. Collectively, our results pointed to the importance of N-linked glycosylation in proteolytic activation of CREB-H.

Unglycosylated CREB-H is less susceptible to ER-localized S1P

The resistance of CREB-H m1+2+3 to BFA-induced proteolytic activation supported the notion that glycosylation primarily affects intramembrane proteolysis, although the possibility of an impact on ER-to-Golgi transport could not be ruled out completely. To further investigate this, we employed the ER-localized S1P in which the transmembrane domain had been replaced by the KDEL tail, an ER retention signal (Chen et al., 2002; Lee et al., 2004; Nadanaka et al., 2007). A non-functional KDAS tail was also included as a negative control (Fig. 9A). If, on the one hand, glycosylation of CREB-H primarily affects ER-to-Golgi transport, KDEL-tailed S1P would be able to activate CREB-H WT and CREB-H m1+2+3 equally. On the other hand, if KDEL-tailed S1P cleaved CREB-H WT preferentially, the proteolysis step is probably most critical. Notably, because S2P cleavage is a rapid process following and induced by S1P cleavage (Zhang et al., 2006; Bailey et al., 2007), the cleaved form of CREB-H detected in our experiment is plausibly the product of both S1P and S2P.

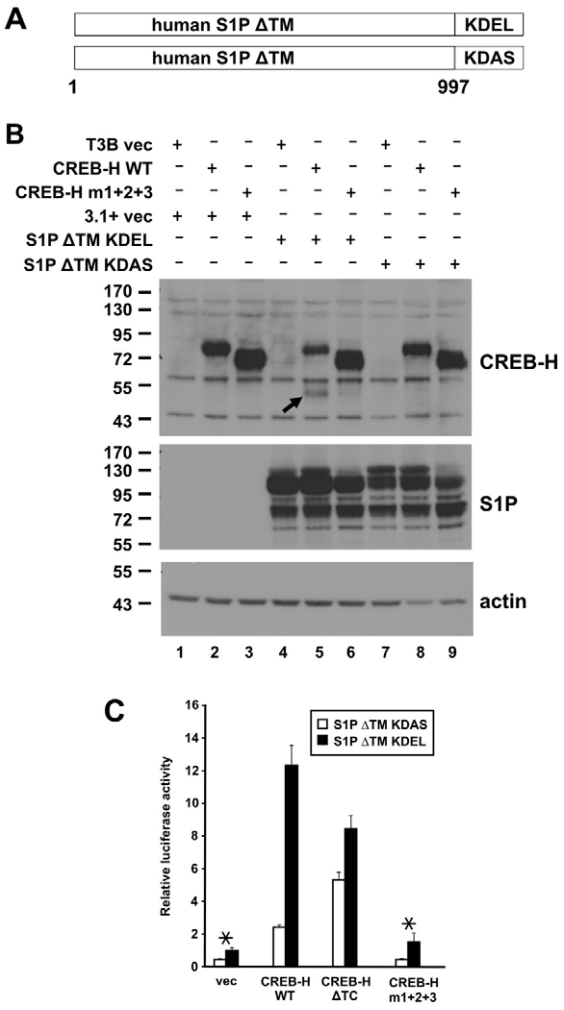

Fig. 9. ER-localized S1P induces proteolytic cleavage and transcriptional activation of CREB-H. (**A**) Schematic representation of recombinant human S1P proteins. The ER-localization signal, KDEL, was fused to human S1PΔTM. The non-functional KDAS sequence served as a control. (**B**) Proteolytic cleavage. HepG2 cells were co-transfected with the indicated combinations of plasmids expressing CREB-H WT, CREB-H m1+2+3, S1PΔTM-KDEL and S1PΔTM-KDAS. pCMV-Tag3B (T3B vec) and pcDNA3.1+ (3.1+ vec) empty vectors were also transfected as controls. Western blotting was performed with α-myc (CREB-H panel), α-V5 (S1P panel) and anti-actin. (**C**) Luciferase assay. Empty vector (vec) and plasmids (0.2 μg each) expressing CREB-H, CREB-HΔTC and CREB-H m1+2+3 were individually co-transfected with pUPRE-Luc reporter plasmid (0.2 μg) and either pcDNA-S1PΔTM-KDEL or pcDNA-S1PΔTM-KDAS plasmid (0.1 μg each) into HepG2 cells. Luciferase activity was assayed as in Fig. 2. Delta analysis was carried out to compare fold activation (S1PΔTM-KDEL versus S1PΔTM-KDAS) in luciferase activity between the empty vector (vec) and CREB-H m1+2+3 groups (*). These two groups are not significantly different (P=0.102, Student's t-test).

Indeed, KDEL-tailed S1P induced proteolysis of CREB-H WT, whereas the cleavage of CREB-H m1+2+3 was minimal (Fig. 9B, lane 5 compared with lane 6). This effect was highly specific since CREB-H WT was not cleaved by KDAS-tailed S1P or empty vector (Fig. 9B, lanes 7-9 and 1-3). The molecular mass (52 kDa) of the CREB-H cleavage product detected (Fig. 9B, lane 5) is consistent with the predicted size of the CREB-H active form produced by S1P and S2P proteases. In line with these results, KDEL-tagged S1P potently activated CREB-H WT-dependent transcription from UPRE, but had minimal stimulatory effect on CREB-H m1+2+3 (Fig. 9C). Therefore, N-linked glycosylation is required primarily for optimal proteolytic activation of CREB-H.

Discussion

In this study, we provided evidence for N-linked glycosylation of CREB-H and demonstrated its requirement for optimal proteolytic activation of CREB-H. CREB-H was N-linked glycosylated at three sites located in its luminal domain at the C-terminal (Fig. 1; supplementary material Fig. S1). An unglycosylated mutant of CREB-H was obtained through disruption of all three sites (Fig. 1) and this mutant was found to be a stable protein (Fig. 3) and a poor activator of transcription from UPRE or CRP promoter (Fig. 2). In addition, unglycosylated CREB-H did not form aggregates in cultured cells (Fig. 5). Even when stimulated with BFA, unglycosylated and deglycosylated CREB-H remained largely uncleaved and inactive in the ER (Figs 6-9; supplementary material Figs S2 and S3). Our findings suggest a new model for regulation of CREB-H activity in which N-linked glycosylation could facilitate intramembrane proteolysis and activation of CREB-H through an as yet unknown mechanism. Although our results contradict previous findings that Tu either stimulates (Zhang et al., 2006) or has no influence (Bailey et al., 2007) on proteolytic activation of CREB-H and we did not understand why similar assays gave different results in three studies. Our demonstration of the inhibitory effect of glycosylation on proteolytic cleavage was based not only on deglycosylated CREB-H obtained after treatment of cells with Tu but also on a new unglycosylated mutant with all glycosylation sites disrupted (Figs 7 and 8). It is noteworthy that all different lines of evidence presented in our study consistently support the notion that N-linked glycosylation is important for optimal proteolytic activation of CREB-H (Figs 2, 4-9; supplementary material Fig. S1-S3).

The modestly decreased transcriptional activity of underglycosylated CREB-H mutants was probably not due to alteration in protein turnover or localization, since their steady-state amounts and subcellular localization remained unchanged (Figs 1 and 3). In addition, partial cleavage and transcriptional activity of unglycosylated CREB-H induced by BFA (Figs 6 and 7) or ER-localized S1P (Fig. 9) indicated the ability of the mutant protein to localize to the ER membrane. Accumulation of unglycosylated CREB-H in the ER did not activate UPRE-dependent transcription (Fig. 2), indicating that it was probably not in an unfolded state. Furthermore, aggregates of unglycosylated CREB-H were not found in either the non-denaturing gel (data not shown) or in cultured cells (Fig. 5). Finally, both unglycosylation of CREB-H caused by the mutation of glycosylation sites and deglycosylation induced by Tu had very similar negative effects on proteolytic cleavage and transcriptional activity (Figs 2, 4, 7, 8; supplementary material Figs S2 and S3). These effects were therefore probably not due to unexpected structural changes as a result of the mutation of asparagines in the luminal domain of CREB-H. Since localization of CREB-H and its mutants to the Golgi complex is transient and the active form of CREB-H is highly unstable (Fig. 6), it is difficult to monitor CREB-H dynamics in the Golgi complex and in the nucleus. Although our data could not completely eliminate the possibility that N-linked glycosylation of CREB-H has an effect on its transport from the ER to the Golgi complex, our results on differential cleavage of CREB-H and its

glycosylation mutant by S1P (Figs 7-9) provided the direct evidence that N-linked glycosylation has an influence on proteolytic activation of CREB-H plausibly after ER-to-Golgi transport.

Although post-translational modifications of proteins are common and may serve regulatory function in various biological contexts (Seet et al., 2006), our demonstration of the requirement of N-linked glycosylation in the luminal domain for proteolytic activation of membrane-bound transcription factors might reveal a new mechanism for transcriptional regulation. This is distinct from all other known examples, in which glycosylation affects DNA binding, coactivator binding, transcriptional activation and other properties of transcription factors (Jackson and Tjian, 1998; Gewinner et al., 2004; Ahmad et al., 2006). It is particularly noteworthy that N-linked glycosylation appears to have opposite impacts on CREB-H and ATF6, another membrane-anchored bZIP transcription factor that plays an important role in UPR (Hong et al., 2004). ATF6 also undergoes N-linked glycosylation at three sites in the luminal domain. However, underglycosylation of ATF6 serves as a sensor of ER homeostasis and induces activation of ATF6. As such, unglycosylated ATF6 is transported more rapidly to the Golgi complex for proteolytic cleavage by S1P and S2P enzymes, leading to constitutive nuclear localization and transcriptional activation in the absence of ER stress (Hong et al., 2004). In sharp contrast, underglycosylation of CREB-H inhibited proteolytic activation and caused a significant decrease in transcriptional activity (Figs 6-9). In addition to other major differences between ATF6 and CREB-H reported in a recent study (Llarena et al., 2010), our findings revealed the differential effects of N-linked glycosylation on CREB-H and ATF6. We did not fully understand the molecular mechanisms underlying these effects. Although both CREB-H and ATF6 can be N-linked glycosylated, they share minimal sequence homology within the luminal domain. In addition, they also respond differentially to inducers of ER stress, such as Tu and Tg (Fig. 4) (Llarena et al., 2010). One possibility is that CREB-H and ATF6 might sense different kinds or levels of stress through their N-linked glycosylation status. Since CREB-H was thought to form a heterodimer with ATF6 (Zhang et al., 2006), further investigations are required to elucidate how an ATF6-CREB-H heterodimer might regulate target gene expression in response to glycosylation inhibitors and UPR stimuli. Notably, a recent report demonstrated that N-linked glycosylation of ATF6β also perturbed proteolytic activation (Guan et al., 2009). Because ATF6β was thought to be a repressor of transcriptionally active ATF6α, this adds another level of complexity to the regulation of ATF6 transcriptional activity by N-linked glycosylation.

Since N-linked glycosylation of CREB-H is important for its proteolytic activation (Figs 2, 6-9), it would be of great interest to understand the regulatory mechanism of CREB-H glycosylation. In this regard, several lines of further investigation might be considered. First, identification of the physiological stimuli of CREB-H glycosylation and deglycosylation might provide valuable information. Particularly, pro-inflammatory cytokines such as TNF-α, IL-1 and IL-6 that induce APR and hepcidin (Moshage, 1997; Vecchi et al., 2009) and other cellular stress signals that stimulate N-linked glycosylation (Lehrman, 2006) should be tested for influence on CREB-H modification and activity. Second, identification and characterization of protein partners that specifically interact with glycosylated CREB-H would shed light on how N-linked glycosylation influences proteolytic cleavage. For example, an escort protein known as SCAP facilitates transport of SREBP from the ER to the Golgi (Goldstein et al., 2006). In the case of ATF6, an interaction with GRP78 is thought to have a role in regulating Golgi localization (Shen et al., 2002; Shen et al., 2005). Although GRP78 has recently been shown to be dispensable for CREB-H activation (Llarena et al., 2010), it would still be of interest to see whether other protein partners such as SCAP might influence the activity of CREB-H. Third, further investigations are required to elucidate how glycosylation of CREB-H is affected by other forms of posttranslational modifications such as phosphorylation and disulfide bond formation. In this regard, it is noteworthy that the formation of disulfide bonds in the luminal domain of ATF6 has been shown to be a sensor of ER stress (Nadanaka et al., 2007). Finally, the analysis of N-linked glycosylation should be extended to other members of the CREB3 subfamily. Although the luminal domains of proteins in the CREB3 subfamily are divergent in sequence, N-linked glycosylation sites are also found within the region. Hence, the regulation of proteolytic activation by N-linked glycosylation probably represents a general mechanism within the CREB3 subfamily.

Another important issue in the characterization of CREB-H is to derive its physiological function in the liver. We have previously suggested CREB-H to be a growth suppressor that is underexpressed in hepatocellular carcinoma (Chin et al., 2005). However, *Crebh*$^{-/-}$ mice were healthy and displayed no overt defects in hepatic development (Luebke-Wheeler et al., 2008). CREB-H has also been shown to cooperate with ATF6 in the activation of APR genes (Zhang et al., 2006). Thus, CREB-H is implicated in both hepatic inflammatory response and carcinogenesis. In this study, potent activation of the CRP promoter by CREB-H was confirmed (Fig. 3). This raises an interesting question as to how N-linked glycosylation of CREB-H might impact the activation of APR genes in the liver.

Our findings that CREB-H is not activated by Tu or Tg (Fig. 6) are not too surprising. Although CREB-H has been shown to be activated by Tu and Tg (Zhang et al., 2006), Tu has also been found to have no effect, or might have a weak inhibitory effect, on proteolytic activation of CREB-H (Bailey et al., 2007). In addition, similar findings on other transcription factors of CREB3 subfamily have also been obtained by different groups. For instance, LZIP, which is closely related to CREB-H, is probably not activated by ER stress or UPR (Chen et al., 2002; Nadanaka et al., 2007). Likewise, proteolytic activation of CREB3L4, another CREB-H-like transcription factor expressed in the prostate, was not induced by Tu (Ben Aicha et al., 2007). In addition, the activation of CREB-H by Tu was either marginal or indirectly demonstrated in two recent studies (Luebke-Wheeler et al., 2008; Vecchi et al., 2009). Thus, further experiments are required to resolve the discrepancies and clarify the physiological stimuli of CREB-H in hepatocytes. In this regard, proinflammatory cytokines such as IL-1β and IL-6 have been suggested to be the physiological inducer of CREB-H activation (Zhang et al., 2006). This has also been independently confirmed by another group [see figure S6 in Bailey et al. (Bailey et al., 2007)]. Exactly how IL-1β and IL-6 induce proteolytic activation of CREB-H, either directly or indirectly, remains to be elucidated.

Materials and Methods

Plasmids

Expression plasmids pcDNA-V5-CREBH and pcDNA-V5-CREBHΔTC have been previously described (Chin et al., 2005). Plasmids for expression of mouse CREB-H glycosylation mutants, m1, m2, m3, m1+2, m1+3, m2+3 and m1+2+3, were created by PCR. In these mutants threonine residues at positions 413, 420 and 427

were mutated to isoleucine individually or in different combinations. Pairs of primers used for T413I (m1), T420I (m2) and T427I (m3) mutagenesis were: 5′-TTGGA CAACC TGATA GAAGA GCTA-3′ and 5′-TAGCT CTTCT ACAGG TTGTC CAA-3′; 5′-CTAGA CAACT CCATC CTGGT GCTG-3′ and 5′-CAGCA CCAGG ATGGA GTTGT CTAG-3′; and 5′-CTGGC CAACT CCATA GAGGA CCTG-3′ and 5′-CAGGT CCTCT ATGGA GTTGG CCAG-3′, respectively. Double and triple mutants were obtained through successive rounds of mutagenesis at targeted positions. Expression plasmids for N-terminally myc-tagged CREB-H glycosylation mutants were constructed by subcloning CREB-H mutant genes into pCMV-Tag3B (Stratagene) via *Eco*RI and *Xho*I restriction sites.

Reporter plasmid pUPRE-Luc has been described elsewhere (Chin et al., 2005) and contains six copies of canonical unfolded protein response element (Wang et al., 2000). Reporter construct pCRP-Luc was derived from pGL3-basic (Promega) and contains –1834 to +150 of the human CRP gene, which was PCR amplified from human genomic clone RP11-419N10 (GenBank AL445528) with primers 5′-CGGGG TACCG TTCTA TCAAG TAGCA GC-3′ and 5′-CCGAC GCGTG ACAGA AGCCA AACTG GA-3′ and inserted via *Kpn*I and *Mlu*I sites.

Expression plasmids pcDNA-hS1PΔTM-KDEL and pcDNA-hS1PΔTM-KDAS were created by PCR amplification of DNA fragments encoding amino acids1-997 of site-1 protease (S1P) from the human cDNA clone (GenBank BC114555) with primers containing sequences that code for KDEL or KDAS at the C-terminus. Pairs of primers used were: 5′-CCGGG ATCCA TGAAG CTTGT CAACA TCTGG C-3′ and 5′-CCGCT CGAGT CATAG CTCGT CCTTC GTAGA ATCGA GACCG AGGA GAGGG TTAGG GATAG GCTTA CCCTC CTGGT TGTAG CGGCC AGGCA T-3′, and 5′-CCGGG ATCCA TGAAG CTTGT CAACA TCTGG C-3′ and 5′-CCGCT CGAGT CAACT GGCGT CCTTC GTAGA ATCGA GACCG AGGAG AGGGT TAGGG ATAGG CTTAC CCTCC TGGTT GTAGC GGCCA GGCAT-3′, respectively. Amplified DNA fragments were then cloned via *Bam*HI and *Xho*I restriction sites into pcDNA3.1+ (Invitrogen) vector with V5 and His tags at the N-terminus. The expression plasmid pcDNA3-ATF6 (Zhu et al., 1997) was kindly provided by Dr Ron Prywes.

Antibodies

Polyclonal antiserum α-CH9 raised against the N-terminal 84 amino acids of mouse CREB-H has been previously described (Chin et al., 2005). The crude antiserum was further purified by pre-adsorbing the anti-glutathione *S*-transferase (GST) antibodies onto a GST-Sepharose column. Rabbit polyclonal anti-V5 and anti-myc were from Sigma and Santa-Cruz, respectively. Mouse monoclonal anti-V5 was from Invitrogen.

Cell culture and transfection

Human hepatoma cell lines HepG2 and Hep3B, human embryonic kidney cell line HEK293T, African green monkey kidney cell line COS-7, and human cervical carcinoma cell line HeLa were grown in Dulbecco's modified Eagle's medium (DMEM) containing 10% fetal bovine serum. Cells were maintained at 37°C in a humidified atmosphere at 5% CO_2. Transfection of cells was carried out as previously described (Kok et al., 2007; Choy et al., 2008a).

Immunoprecipitation

Fresh mouse liver tissue was obtained and homogenized in ice-cold non-denaturing lysis buffer (20 mM Tris-HCl, pH 8.0, 150 mM NaCl, 10% glycerol, 1% NP-40) in the presence of protease inhibitor cocktail (Roche) for 1 minute. Homogenized tissue was lysed for 30 minutes on ice. Cell debris was removed by centrifugation at 16,000 ***g*** at 4°C. Lysates were then pre-cleared by rocking with rProtein-A-Sepharose fast flow beads (Amersham) for 1 hour at 4°C. After pre-clearing, the lysates were rocked for another 2 hour with beads that had been pre-incubated for 1 hour with α-CH9 and washed twice after incubation. After protein binding to α-CH9, beads were washed four times.

Western blotting

Cells were lysed with lysis buffer (50 mM Tris-HCl, pH 7.4, 150 mM NaCl, 1% Triton X-100, 0.1% SDS, 1% sodium deoxycholate, 2 mM PMSF, 5 mM NaF, 0.5 mM sodium vanadate, 0.5 mM EDTA, 1% NP40) supplemented with protease inhibitors (Roche). Samples containing equal amounts of protein were separated by SDS-PAGE and electroblotted onto Immobilon-P membranes (Millipore) using Hoefer SemiPhor semi-dry blotting apparatus (Amersham). Blots were blocked with 5% skimmed milk, followed by incubation with primary antibodies. Blots were then incubated with goat anti-rabbit or anti-mouse secondary antibody conjugated to horseradish peroxidase (Amersham) and visualized by enhanced chemiluminescence (Amersham) as described previously (Chin et al., 2007a; Chin et al., 2007b; Siu et al., 2008).

For endoglycosidase treatment, cell lysates were incubated with Endo-H (1 IU/μg protein; New England Biolabs) or PNGase F (1 IU/μg protein; New England Biolabs) for 2 hours at 37°C. For brefeldin A (BFA) treatment, cells were incubated with 5 μg/ml BFA (Calbiochem) for 6 hours before harvest. For MG-132 treatment, cells were incubated with 10 μM MG-132 (Calbiochem) for 4 hours before harvest. For cycloheximide treatment, 200 μM cycloheximide (Sigma-Aldrich) was used. For tunicamycin (Tu) treatment, cells were incubated with 2 μg/ml Tu for 4 hours. For thapsigargin (Tg) treatment, cells were incubated with 300 nM Tg for 16 hours.

Reporter assays

HepG2 and Hep3B cells were cultured in DMEM and transfected using Genejuice transfection reagent (EMD Chemicals). Cells were harvested 48 hours after transfection. Luciferase activity was determined as previously described (Ching et al., 2006; Siu et al., 2006) using dual luciferase reagents (Promega). Transcriptional activity on unfolded protein response element (UPRE) and C-reactive protein (CRP) promoter was measured with plasmids pUPRE-Luc and pCRP-Luc, respectively. Transfection efficiencies were normalized using a control plasmid (pSV-RLuc from Promega) expressing *Renilla* luciferase. Luminescence was measured with a LB9570 luminometer (EG&G).

RT-PCR analysis

HepG2 cells were harvested 48 hours after transfection. Total RNA was extracted with Trizol reagent (Invitrogen). RNA samples were then treated with DNase I (Ambion) to remove contaminating genomic DNA. Next, 5 μg of RNA were used for cDNA synthesis using Thermoscript RT-PCR reagents (Invitrogen) and oligo$(dT)_{20}$ primer. PCR was performed as previously described (Choy et al., 2008b; Tang et al., 2009) using cDNA as template. PCR products were separated by 2% agarose gel electrophoresis. Primer pairs for PCR of CRP and β-actin were: 5′-GAACT TTCAG CCGAA TACAT CTTTT-3′ and 5′-GTGGC ATACG AGAAA ATACT GTACC-3′, and 5′-ATCTG GCACC ACACC TTCTAC-3′ and 5′-AGTAC TTGCG CTCAG GAGGA-3′, respectively.

Confocal microscopy

Multicolour immunofluorescence imaging was performed on a Zeiss LSM510 confocal microscope as previously described (Chan et al., 2006; Siu et al., 2009a; Siu et al., 2009b). HeLa cells were fixed and permeabilized with ice cold methanol:acetone (1:1) for 5 minutes. Cells were blocked with 3% bovine serum albumin (BSA) for 1 hour. Cells were incubated with primary and conjugated secondary antibodies for 1 hour individually in 3% BSA. Nuclei were counter stained with 0.5 μg/ml 4′,6-diamidino-2-phenylindole (DAPI) before mounting.

We thank Ron Prywes for the pcDNA3-ATF6 plasmid, and Wilson Ching, Abel Chun, Raven Kok, James Ng, Kam-Leung Siu, Ken Siu, Vincent Tang and Chi-Ming Wong for critical reading of the manuscript. The study was supported by grants HKU 7486/06M and HKU 1/06C from the Hong Kong Research Grants Council.

Supplementary material available online at
http://jcs.biologists.org/cgi/content/full/123/9/1438/DC1

References

Ahmad, I., Hoessli, D. C., Walker-Nasir, E., Rafik, S. M., Shakoori, A. R. and Nasir-ud-Din. (2006). Oct-2 DNA binding transcription factor: functional consequences of phosphorylation and glycosylation. *Nucleic Acids Res.* **34**, 175-184.

Bachmair, A., Finley, D. and Varshavsky, A. (1986). *In vivo* half-life of a protein is a function of its amino-terminal residue. *Science* **234**, 179-186.

Bailey, D. and O'Hare, P. (2007). Transmembrane bZIP transcription factors in ER stress signaling and the unfolded protein response. *Antioxid. Redox Sign.* **9**, 2305-2322.

Bailey, D., Barreca, C. and O'Hare, P. (2007). Trafficking of the bZIP transmembrane transcription factor CREB-H into alternate pathways of ERAD and stress-regulated intramembrane proteolysis. *Traffic* **8**, 1796-1814.

Bause, E. (1983). Structural requirements of N-glycosylation of proteins. Studies with proline peptides as conformational probes. *Biochem. J.* **209**, 331-336.

Ben Aicha, S., Lessard, J., Pelletier, M., Fournier, A., Calvo, E. and Labrie, C. (2007). Transcriptional profiling of genes that are regulated by the endoplasmic reticulum-bound transcription factor AIbZIP/CREB3L4 in prostate cells. *Physiol. Genomics* **31**, 295-305.

Bengoechea-Alonso, M. T. and Ericsson, J. (2007). SREBP in signal transduction: cholesterol metabolism and beyond. *Curr. Opin. Cell Biol.* **19**, 215-222.

Brown, M. S. and Goldstein, J. L. (1997). The SREBP pathway: regulation of cholesterol metabolism by proteolysis of a membrane-bound transcription factor. *Cell* **89**, 331-340.

Brown, M. S., Ye, J., Rawson, R. B. and Goldstein, J. L. (2000). Regulated intramembrane proteolysis: a control mechanism conserved from bacteria to humans. *Cell* **100**, 391-398.

Chan, C. P., Siu, K. L., Chin, K. T., Yuen, K. Y., Zheng, B. and Jin, D. Y. (2006). Modulation of the unfolded protein response by severe acute respiratory syndrome coronavirus spike protein. *J. Virol.* **80**, 9279-9287.

Chen, X., Shen, J. and Prywes, R. (2002). The luminal domain of ATF6 senses endoplasmic reticulum (ER) stress and causes translocation of ATF6 from the ER to the Golgi. *J. Biol. Chem.* **277**, 13045-13052.

Chin, K. T., Zhou, H. J., Wong, C. M., Lee, J. M., Chan, C. P., Qiang, B. Q., Yuan, J. G., Ng, I. O. L. and Jin, D. Y. (2005). The liver-enriched transcription factor CREB-H is a growth suppressor protein underexpressed in hepatocellular carcinoma. *Nucleic Acids Res.* **33**, 1859-1873.

Chin, K. T., Chun, A. C. S., Ching, Y. P., Jeang, K. T. and Jin, D. Y. (2007a). Human T-cell leukemia virus oncoprotein Tax represses nuclear receptor-dependent transcription by targeting coactivator TAX1BP1. *Cancer Res.* **67**, 1072-1081.

Chin, K. T., Xu, H. T., Ching, Y. P. and Jin, D. Y. (2007b). Differential subcellular localization and activity of kelch repeat proteins KLHDC1 and KLHDC2. *Mol. Cell. Biochem.* **296**, 109-119.

Ching, Y. P., Chan, S. F., Jeang, K. T. and Jin, D. Y. (2006). Retroviral oncoprotein Tax targets coiled-coil centrosomal protein TAX1BP2 to induce centrosome overduplication. *Nat. Cell Biol.* **8**, 717-724.

Choy, E. Y. W., Kok, K. H., Tsao, S. W. and Jin, D. Y. (2008a). Utility of Epstein-Barr virus-encoded small RNA promoters for driving the expression of fusion transcripts harboring small hairpin RNAs. *Gene Ther.* **15**, 191-202.

Choy, E. Y. W., Siu, K. L., Kok, K. H., Lung, R. W. M., Tsang, C. M., To, K. F., Kwong, D. L. W., Tsao, S. W. and Jin, D. Y. (2008b). An Epstein-Barr virus-encoded microRNA targets PUMA to promote host cell survival. *J. Exp. Med.* **205**, 2551-2560.

Costa, R. H., Kalinichenko, V. V., Holterman, A. X. and Wang, X. (2003). Transcription factors in liver development, differentiation, and regeneration. *Hepatology* **38**, 1331-1347.

Duncan, S. A. (2000). Transcriptional regulation of liver development. *Dev. Dyn.* **219**, 131-142.

Freiman, R. N. and Herr, W. (1997). Viral mimicry: common mode of association with HCF by VP16 and the cellular protein LZIP. *Genes Dev.* **11**, 3122-3127.

Gabay, C. and Kushner, I. (1999). Acute-phase proteins and other systemic responses to inflammation. *New Engl. J. Med.* **340**, 448-454.

Gewinner, C., Hart, G., Zachara, N., Cole, R., Beisenherz-Huss, C. and Groner, B. (2004). The coactivator of transcription CREB-binding protein interacts preferentially with the glycosylated form of Stat5. *J. Biol. Chem.* **279**, 3563-3572.

Goldstein, J. L., DeBose-Boyd, R. A. and Brown, M. S. (2006). Protein sensors for membrane sterols. *Cell* **124**, 35-46.

Guan, D., Wang, H., Li, V. E., Xu, Y., Yang, M. and Shen, Z. (2009). N-glycosylation of ATF6β is essential for its proteolytic cleavage and transcriptional repressor function to ATF6α. *J. Cell. Biochem.* **108**, 825-831.

Haze, K., Yoshida, H., Yanagi, H., Yura, T. and Mori, K. (1999). Mammalian transcription factor ATF6 is synthesized as a transmembrane protein and activated by proteolysis in response to endoplasmic reticulum stress. *Mol. Biol. Cell* **10**, 3787-3799.

Hong, M., Luo, S., Baumeister, P., Huang, J. M., Gogia, R. K., Li, M. and Lee, A. S. (2004). Underglycosylation of ATF6 as a novel sensing mechanism for activation of the unfolded protein response. *J. Biol. Chem.* **279**, 11354-11363.

Jackson, S. P. and Tjian, R. (1988). O-glycosylation of eukaryotic transcription factors: implications for mechanisms of transcriptional regulation. *Cell* **55**, 125-133.

Jin, D. Y., Wang, H. L., Zhou, Y., Chun, A. C., Kibler, K. V., Hou, Y. D., Kung, H. and Jeang, K. T. (2000). Hepatitis C virus core protein-induced loss of LZIP function correlates with cellular transformation. *EMBO J.* **19**, 729-740.

Kane, R., Murtagh, J., Finlay, D., Marti, A., Jaggi, R., Blatchford, D., Wilde, C. and Martin, F. (2002). Transcription factor NFIC undergoes N-glycosylation during early mammary gland involution. *J. Biol. Chem.* **277**, 25893-25903.

Kok, K. H., Ng, M. H., Ching, Y. P. and Jin, D. Y. (2007). Human TRBP and PACT interact with each other and associate with Dicer to facilitate the production of small interfering RNA. *J. Biol. Chem.* **282**, 17649-17657.

Kondo, S., Murakami, T., Tatsumi, K., Ogata, M., Kanemoto, S., Otori, K., Iseki, K., Wanaka, A. and Imaizumi, K. (2005). OASIS, a CREB/ATF family member, modulates UPR signalling in astrocytes. *Nat. Cell Biol.* **7**, 186-194**.**

Kondo, S., Saito, A., Hino, S., Murakami, T., Ogata, M., Kanemoto, S., Nara, S., Yamashita, A., Yoshinaga, K., Hara, H. et al. (2007). BBF2H7, a novel transmembrane bZIP transcription factor, is a new type of ER stress transducer. *Mol. Cell. Biol.* **27**, 1716-1729.

Lamarre-Vincent, N. and Hsieh-Wilson, L. C. (2003). Dynamic glycosylation of the transcription factor CREB: a potential role in gene regulation. *J. Am. Chem. Soc.* **125**, 6612-6613.

Lee, M. C. S., Miller, E. A., Goldberg, J., Orci, L. and Schekman, R. (2004). Bi-directional protein transport between the ER and Golgi. *Annu. Rev. Cell Dev. Biol.* **20**, 87-123.

Lee, P. L. and Beutler, E. (2009). Regulation of hepcidin and iron-overloaded disease. *Annu. Rev. Pathol. Mech. Dis.* **4**, 489-515.

Lehrman, M. A. (2006). Stimulation of N-linked glycosylation and lipid-linked oligosaccharide synthesis by stress responses in metazoan cells. *Crit. Rev. Biochem. Mol. Biol.* **41**, 51-75.

Lippincott-Schwartz, J., Yuan, L. C., Bonifacino, J. S. and Klausner, R. D. (1989). Rapid redistribution of Golgi proteins into the ER in cells treated with brefeldin A: Evidence for membrane cycling from Golgi to ER. *Cell* **56**, 801-813.

Llarena, M., Bailey, D., Curtis, H. and O'Hare, P. (2010). Different mechanisms of recognition and ER retention by transmembrane transcription factors CREB-H and ATF6. *Traffic* **11**, 48-69.

Lu, R., Yang, P., O'Hare, P. and Misra, V. (1997). Luman, a new member of the CREB/ATF family, binds to herpes simplex virus VP16-associated host cellular factor. *Mol. Cell. Biol.* **17**, 5117-5126.

Luebke-Wheeler, J., Zhang, K., Battle, M., Si-Tayeb, K., Garrison, W., Chhinder, S., Li, J., Kaufman, R. J. and Duncan, S. A. (2008). Hepatocyte nuclear factor 4α is implicated in endoplasmic reticulum stress-induced acute phase response by regulating expression of cyclic adenosine monophosphate responsive element binding protein H. *Hepatology* **48**, 1242-1250.

Mortensen, R. F. (2001). C-reactive protein, inflammation, and innate immunity. *Immunol. Res.* **24**, 163-176.

Moshage, H. (1997). Cytokines and the hepatic acute phase response. *J. Pathol.* **181**, 257-266.

Murakami, T., Saito, A., Hino, S., Kondo, S., Kanemoto, S., Chihara, K., Sekiya, H., Tsumagari, K., Ochiai, K., Yoshinaga, K. et al. (2009). Signalling mediated by the endoplasmic reticulum stress transducer OASIS is involved in bone formation. *Nat. Cell Biol.* **11**, 1205-1211.

Nadanaka, S., Okada, T., Yoshida, H. and Mori, K. (2007). Role of disulfide bridges formed in the luminal domain of ATF6 in sensing endoplasmic reticulum stress. *Mol. Cell. Biol.* **27**, 1027-1043.

Nishikawa, T., Hagihara, K., Serada, S., Isobe, T., Matsumura, A., Song, J., Tanaka, T., Kawase, I., Naka, T. and Yoshizaki, K. (2008). Transcriptional complex formation of c-Fos, STAT3, and hepatocyte NF-1α is essential for cytokine-driven C-reactive protein gene expression. *J. Immunol.* **180**, 3492-3501.

Omori, Y., Imai, J., Watanabe, M., Komatsu, T., Suzuki, Y., Kataoka, K., Watanabe, S., Tanigami, A. and Sugano, S. (2001). CREB-H: a novel mammalian transcription factor belonging to the CREB/ATF family and functioning via the box-B element with a liver-specific expression. *Nucleic Acids Res.* **29**, 2154-2162.

Raggo, C., Rapin, N., Stirling, J., Gobeil, P., Smith-Windsor, E., O'Hare, P. and Misra, V. (2002). Luman, the cellular counterpart of herpes simplex virus VP16, is processed by regulated intramembrane proteolysis. *Mol. Cell. Biol.* **22**, 5639-5649.

Ron, D. and Walter, P. (2007). Signal integration in the endoplasmic reticulum unfolded protein response. *Nat. Rev. Mol. Cell Biol.* **8**, 519-529.

Saito, A., Hino, S., Murakami, T., Kanemoto, S., Kondo, S., Saitoh, M., Nishimura, R., Yoneda, T., Furuichi, T., Ikegawa, S., et al. (2009). Regulation of endoplasmic reticulum stress response by a BBF2H7-mediated Sec23a pathway is essential for chondrogenesis. *Nat. Cell Biol.* **11**, 1197-1204.

Schrem, H., Klempnauer, J. and Borlak, J. (2002). Liver-enriched transcription factors in liver function and development. Part I: the hepatocyte nuclear factor network and liver-specific gene expression. *Pharmacol. Rev.* **54**, 129-158.

Schrem, H., Klempnauer, J. and Borlak, J. (2004). Liver-enriched transcription factors in liver function and development. Part II: the C/EBPs and D site-binding protein in cell cycle control, carcinogenesis, circadian gene regulation, liver regeneration, apoptosis, and liver-specific gene regulation. *Pharmacol. Rev.* **56**, 291-330.

Seet, B. T., Dikic, I., Zhou, M. M. and Pawson, T. (2006). Reading protein modifications with interaction domains. *Nat. Rev. Mol. Cell Biol.* **7**, 473-483.

Shen, J., Chen, X., Hendershot, L. and Prywes, R. (2002). ER stress regulation of ATF6 localization by dissociation of BiP/GRP78 binding and unmasking of Golgi localization signals. *Dev. Cell* **3**, 99-111.

Shen, J., Snapp, E. L., Lippincott-Schwartz, J. and Prywes, R. (2005). Stable binding of ATF6 to BiP in the endoplasmic reticulum stress response. *Mol. Cell. Biol.* **25**, 921-932.

Siu, Y. T., Chin, K. T., Siu, K. L., Choy, E. Y. W., Jeang, K. T. and Jin, D. Y. (2006). TORC1 and TORC2 coactivators are required for Tax activation of the human T-cell leukemia virus type 1 long terminal repeats. *J. Virol.* **80**, 7052-7059.

Siu, Y. T., Ching, Y. P. and Jin, D. Y. (2008). Activation of TORC1 transcriptional coactivator through MEKK1-induced phosphorylation. *Mol. Biol. Cell* **19**, 4750-4761.

Siu, K. L., Kok, K. H., Ng, M. H. J., Poon, V. K. M., Yuen, K. Y., Zheng, B. J. and Jin, D. Y. (2009a). Severe acute respiratory syndrome coronavirus M protein inhibits type I interferon production by impeding the formation of TRAF3.TANK.TBK1/IKKε complex. *J. Biol. Chem.* **284**, 16202-16209.

Siu, K. L., Chan, C. P., Chan, C., Zheng, B. J. and Jin, D. Y. (2009b). Severe acute respiratory syndrome coronavirus nucleocapsid protein does not modulate transcription of human *FGL2* gene. *J. Gen. Virol.* **90**, 2107-2113.

Stirling, J. and O'Hare, P. (2006). CREB4, a transmembrane bZip transcription factor and potential new substrate for regulation and cleavage by S1P. *Mol. Biol. Cell* **17**, 413-426.

Tang, H. M. V., Siu, K. L., Wong, C. M. and Jin, D. Y. (2009). Loss of yeast peroxiredoxin Tsa1p induces genome instability through activation of DNA damage checkpoint and elevation of dNTP levels. *PLoS Genet.* **5**, e1000697.

Vecchi, C., Montosi, G., Zhang, K., Lamberti, I., Duncan, S. A., Kaufman, R. J. and Pietrangelo, A. (2009). ER stress controls iron metabolism through induction of hepcidin. *Science* **325**, 877-880.

Vinson, C., Acharya, A. and Taparowsky, E. J. (2006). Deciphering B-ZIP transcription factor interactions *in vitro* and *in vivo*. *Biochim. Biophys. Acta* **1759**, 4-12.

Wang, Y., Shen, J., Arenzana, N., Tirasophon, W., Kaufman, R. J. and Prywes, R. (2000). Activation of ATF6 and an ATF6 DNA binding site by the endoplasmic reticulum stress response. *J. Biol. Chem.* **275**, 27013-27020.

Ye, J., Rawson, R. B., Komuro, R., Chen, X., Davé, U. P., Prywes, R., Brown, M. S. and Goldstein, J. L. (2000). ER stress induces cleavage of membrane-bound ATF6 by the same proteases that process SREBPs. *Mol. Cell* **6**, 1355-1364.

Zhang, K., Shen, X., Wu, J., Sakaki, K., Saunders, T., Rutkowski, D. T., Back, S. H. and Kaufman, R. J. (2006). Endoplasmic reticulum stress activates cleavage of CREBH to induce a systemic inflammatory response. *Cell* **124**, 587-599.

Zhu, C., Johansen, F. E. and Prywes, R. (1997). Interaction of ATF6 and serum response factor. *Mol. Cell. Biol.* **17**, 4957-4966.